

# **FFI RAPPORT**

## **MODELLING THE THERMAL SIGNATURE OF NATURAL BACKGROUNDS**

OLSEN Frode Berg, GAMBORG Marius

**FFI/RAPPORT-2001/05324**



FFIE/775/119.2

Approved  
Kjeller 10. December 2002

Stian Løvold  
Director of Research

**MODELLING THE THERMAL SIGNATURE OF  
NATURAL BACKGROUNDS**

OLSEN Frode Berg, GAMBORG Marius

FFI/RAPPORT-2001/05324

**FORSVARETS FORSKNINGSINSTITUTT**  
**Norwegian Defence Research Establishment**  
P O Box 25, NO-2027 Kjeller, Norway



P O BOX 25  
 NO-2027 KJELLER, NORWAY  
**REPORT DOCUMENTATION PAGE**

**SECURITY CLASSIFICATION OF THIS PAGE**  
 (when data entered)

1) PUBL/REPORT NUMBER FFI/RAPPORT-2001/05324	2) SECURITY CLASSIFICATION UNCLASSIFIED	3) NUMBER OF PAGES 31
1a) PROJECT REFERENCE FFIE/775/119.2	2a) DECLASSIFICATION/DOWNGRADING SCHEDULE -	
4) TITLE MODELLING THE THERMAL SIGNATURE OF NATURAL BACKGROUNDS		
5) NAMES OF AUTHOR(S) IN FULL (surname first) OLSEN Frode Berg, GAMBORG Marius		
6) DISTRIBUTION STATEMENT Approved for public release. Distribution unlimited. (Offentlig tilgjengelig)		
7) INDEXING TERMS IN ENGLISH:		
a) <u>Thermal signatures</u>		IN NORWEGIAN:
b) <u>Natural surfaces</u>		a) <u>Termisk signatur</u>
c) <u>Meteorological parameters</u>		b) <u>Naturoverflater</u>
d) <u>Surface temperatures</u>		c) <u>Meteorologiske parametere</u>
e) <u>Mathematical formulation</u>		d) <u>Overflatetemperaturer</u>
		e) <u>Matematisk formulering</u>
THESAURUS REFERENCE:		
8) ABSTRACT <p>A model for calculation of surface temperatures of different background elements like edge of forest, heather, rock and gravel has been developed. The model is based on a simple mathematical description of the physical processes involved in heat transfer to and from an outdoors natural surface. The same model is used for all background elements, but with different sets of model parameters.</p> <p>Example calculations for edge of forest and rock have been given, showing very good agreement with measured surface temperatures. For the example calculations, the model parameters have been estimated by fitting the model to measured surface temperatures. Finally, the model sensitivity to changes in model parameters have been discussed and it has been demonstrated that the model performs well even with model parameters estimated from datasets obtained at different geographical locations.</p>		
9) DATE 10. December 2002	AUTHORIZED BY This page only Stian Løvold	POSITION Director of Research

ISBN-82-464-0701-5

**UNCLASSIFIED**

**SECURITY CLASSIFICATION OF THIS PAGE**  
 (when data entered)



**CONTENTS**

	<b>Page</b>	
1	INTRODUCTION	7
2	THE THERMAL SIGNATURE MODEL	7
2.1	A mathematical formulation of the physical processes	7
2.2	Solving the differential equations	9
2.3	Estimating the model parameters	10
3	MODEL VALIDATION	11
3.1	Measured background temperatures and environmental data	11
3.2	Example calculations	12
3.2.1	General simplifications	12
3.2.2	Edge of forest	12
3.2.3	Rock	14
3.2.4	Model parameters	16
3.3	Model results	17
3.4	Parameter sensitivity	17
3.5	Model validity	19
3.6	Effect of the individual parameters	20
4	SUMMARY	23
APPENDIX		
A	HEAT CONDUCTION	24
A.1	Difference formulae for heat conduction	24
A.2	Heat conduction with sinusoidal temperature variations	26
A.3	Calculation of damping depth based on measurements by the rock temperature sensor	27
A.4	Calculation of damping per layer	28
	References	30
	Distribution list	31



## MODELLING THE THERMAL SIGNATURE OF NATURAL BACKGROUNDS

### 1 INTRODUCTION

FFI-project 775 “Reduction of thermal signatures” (1) had as goal to establish a mathematical model for calculation of temperatures of natural surfaces such as edge of forest, grass, heather, gravel etc. This was an ambitious goal, but based on successful work on similar models by FGAN-FOM (2) the main challenge was regarded to be the collection of environmental data and measurements of surface temperatures for input and validation of the model.

This paper describes the model and its validation against real measured surface temperatures. One single model is used for different types of background elements but with different sets of model parameters for each background type. The model is validated against data from the southern and northern parts of Norway (Rygge and Bardufoss respectively) where the project had established measuring stations for the purpose of collecting input and validation data for the model (3).

### 2 THE THERMAL SIGNATURE MODEL

#### 2.1 A mathematical formulation of the physical processes

The discussion in this section very much follows Leidner, Clement and Jessen (2).

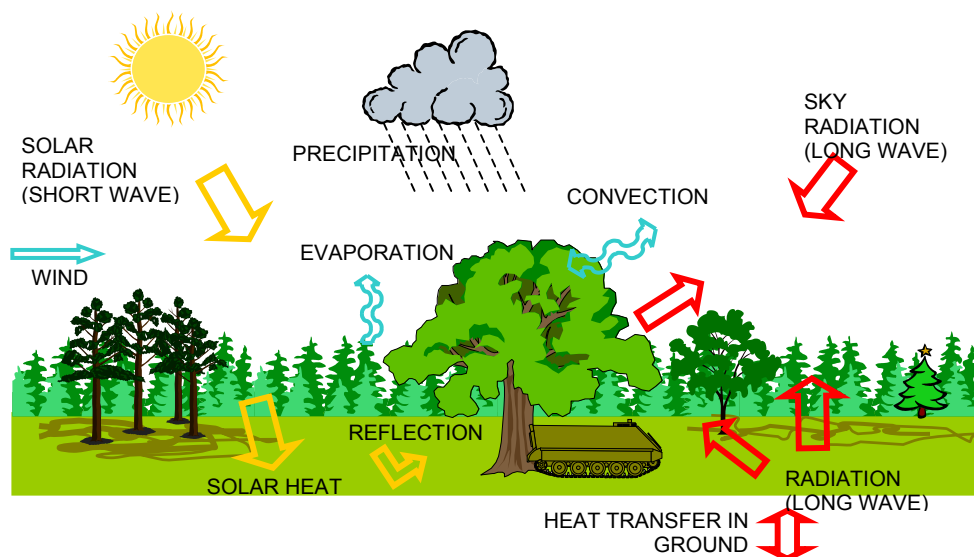


Figure 2.1 Processes influencing the temperature of natural surfaces.

An outdoor surface absorbs radiation from the sun, the sky and the surroundings (see Figure 2.1). In addition the surface exchanges heat with the surrounding air either by wind (forced convection) or by circulation of the air at the surface due to temperature differences between the surface and the air (free convection). If the surface is moist, it is cooled when the water vaporizes, and if the surface is colder than the air, condensation of the air humidity may occur and contribute to heating of the surface. For surfaces of rock, soil etc. heat conduction in the ground may act as a heat source or heat sink depending on the temperature profile in the ground.

The model described below is based on the mentioned processes for heat transfer to and from a surface. In order to make the model as simple as possible, but without ignoring important contributions to the heat balance, the model is formulated as a one-dimensional heat transfer problem. That is, the model is described as a number of stacked layers, where only the upper layer exchanges heat with the surroundings. The only mechanism for heat transfer between the layers is conduction. This means that the model discards heat transported by water flowing down into the ground and also evaporation and diffusion of stored water.

The change in surface temperature during a period of time depends on the heat capacity of the surface and on the net heat flow to the surface. This is expressed by the equation below

$$\frac{dT}{dt}C = Q + L + V + B, \quad (2.1)$$

where  $C$  is the heat capacity of the surface, and  $Q$ ,  $L$ ,  $V$  and  $B$  are radiative heat flux, sensible heat flux, latent heat flux and conductive heat flux respectively.

The radiative heat flux is a sum of radiative heat terms: absorption of global solar radiation  $W_{\text{sun}}$ , absorption of down welling long wave atmospheric radiation  $W_{\text{sky}}$  and long wave radiation emitted by the surface of temperature  $T_s$  as described by Stefan-Boltzmann's law:

$$Q = \alpha W_{\text{sun}} + \varepsilon W_{\text{sky}} + \varepsilon \sigma T_s^4. \quad (2.2)$$

In the above expression  $\alpha$  is the solar absorptance (short wave),  $\varepsilon$  is thermal emissivity (long wave), and  $\sigma$  is the Stefan-Boltzmann constant. By the use of Kirchhoff's law the thermal emissivity has replaced the long wave absorptance.

The sensible heat flux is a sum of terms describing free and forced convection:

$$L = (h_1 + h_2 v_a)(T_a - T_s), \quad (2.3)$$

where  $h_1$  and  $h_2$  are the coefficients of free and forced convection respectively,  $v_a$  is the wind velocity and  $T_a$  is the air temperature.

Analogously, the latent heat exchange term is written:

$$V = r(h_1 + h_2 v_a)(e(T_a, rh) - e(T_s, 100\%)), \quad (2.4)$$

where  $e(T, rh)$  is the water vapour pressure at temperature  $T$  (in hPa),  $rh$  is the relative humidity (in %) and  $r$  is a free parameter describing the ratio between the sensible and latent heat convective coefficients.

The last term in (2.1), the heat conduction term  $B$  represents heat conduction between the layers:

$$B = \kappa \Delta T, \quad (2.5)$$

where  $\kappa$  is the thermal conductivity of the layer and  $\Delta T$  is the temperature difference between two neighbouring layers. The heat conduction term is only considered for “solid” background elements like rock and gravel. For “non-solid” elements like the edge of forest and heather, internal heat conduction is ignored.

Writing out all the terms in (2.1) and taking into account internal heat conduction, the problem becomes a system of  $N$  coupled differential equations, as shown in (2.6).

$$\begin{aligned} \frac{dT_s}{dt} C &= \alpha W_{\text{sun}} + \varepsilon W_{\text{sky}} - \varepsilon \sigma T_s^4 \\ &\quad - (h_1 + h_2 v_a)(T_s - T_a) \\ &\quad + r(h_1 + h_2 v_a)(e(T_a, rh) - e(T_s, 100\%)) \\ &\quad + \kappa(T_1 - T_s) \\ L & \end{aligned} \quad (2.6)$$

$$\frac{dT_i}{dt} C = \kappa(T_{i+1} - 2T_i + T_{i-1})$$

L

$$\frac{dT_N}{dt} C = \kappa(T_c - 2T_N + T_{N-1})$$

In (2.6)  $N$  is the number of layers used and  $T_c$  the temperature of the last layer. This can be a constant core temperature, or a temperature varying with the seasons, but being independent of short-term fluctuations in the weather (4). For more details on heat conduction see appendix A.

## 2.2 Solving the differential equations

In order to solve the system of  $N$  coupled differential equations, the time derivative operator is replaced by a difference operator. In (2.7) below a more compact formulation is introduced where  $T_i$  is the temperature of layer  $i$  (the first layer being the surface layer),  $\vec{T}$  is the array of temperatures  $T_i$ ,  $\vec{\alpha}$  is the array of free model parameters,  $\vec{W}$  is the “weather” i.e. solar load, wind speed etc as described in section 2.1 above.  $F_i$  are the functions on the right hand side of the equations in (2.6).



$$T_i(t+\Delta t) = T_i(t) + F_i(\bar{\alpha}, \bar{W}(t), \bar{T}(t)) \Delta t \quad (2.7)$$

Using this equation the temperatures of the layers can be calculated in a stepping algorithm. To start the algorithm a reasonable surface temperature and temperature profile ( $T_1, \dots, T_N, T_c$ ) must be given. Experience has shown that the model converges to measured temperatures after calculating the temperatures for a two hour long period depending on the quality of the starting values and the time step  $\Delta T$ .

Since the functions  $F_i$  generally are non-linear in  $T$ , the time step is a critical parameter in the stepping algorithm. As a starting point, the model was used with 30s time intervals. Since the environmental data  $\bar{W}$  was recorded with 5 min intervals, linear interpolation was used between the samples to produce input for every time step. This will be discussed further in section 3.2.

### 2.3 Estimating the model parameters

The surface temperatures can be calculated by (2.7) when the model parameters and starting conditions are given. The model can be applied on a variety of surfaces with the model parameters varying from type to type. Theoretically, the model parameters could be measured or found in literature, but in practice this is not feasible. Instead the parameters can be determined by finding the values that gives the best possible agreement between calculated and measured temperatures.

The most commonly used measure of “goodness of fit” is the sum of squares:

$$X^2 = \sum_i (T_{\text{meas}}(t_i) - T_{\text{calc}}(t_i))^2 \quad (2.8)$$

where  $T_{\text{calc}}^o(t_i)$  is the calculated surface temperature and  $T_{\text{meas}}^o(t_i)$  is the measured temperature at time step  $i$ . Using this method the model parameters that minimize the function  $X^2$  are to be found. If the function to be minimized is linear in the parameters to be determined, this is normally done by the method of linear regression. In the case of (2.7) linearity is not generally true and other methods have to be applied.

One method that almost always works, and often is considered the best method to use simply because it is reliable and easy to implement, is the downhill simplex method (5)(6). The method uses a special geometrical object, the “simplex”, which “rolls downhill” to the minimum point of  $X^2$ . The method is not very fast, but has the advantage that it does not require the computation of the derivatives of  $X^2$ .

Another method that is very effective is the Levenberg-Marquardt method (6). This method is specifically tailored for non-linear least squares problems. Unlike the simplex method it requires the estimation of the partial derivatives of the  $X^2$  with respect to each of the parameters in the model. This method is faster than the simplex method, but it diverges more often. Often a combination of the two methods will give the best results.

In the calculations presented in this paper, an implementation of both these methods in the computer library “MFXMLibs Numerical Library” from Math Soft Inc is used.

### 3 MODEL VALIDATION

#### 3.1 Measured background temperatures and environmental data

To collect real environmental data for input to the model, two measuring stations were established, one in the northern part of Norway (Bardufoss, 69°3’N, 18°34’E) and one in the southern part (Rygge, 59°24’N, 10°43’E). The measuring sites were chosen to give a large variation in measured meteorological conditions. At Rygge warm summers and mild winters are expected and at Bardufoss midnight sun and polar night conditions are measured. The measuring stations are described in detail in (3).

At the measuring stations standard meteorological parameters such as air temperature, wind speed, relative humidity, in and out welling global and long wave radiation and precipitation are measured. The parameters are measured every 30s and moving averages are stored every 5 minutes.

In addition to environmental data, measured surface temperatures are needed to calibrate and validate the model. For this purpose, thermal images of the surroundings close to the meteorological measuring stations were recorded every 15 minutes. The thermal camera was internally calibrated and had a nominal temperature resolution better than 0.1K, and operates in the 8-12  $\mu\text{m}$  band.

In the stored thermal imagery the apparent temperature of every pixel can be calculated, and this was used to calculate the mean temperatures of regions containing background elements like edge of forest, heather, gravel and rock. Examples of such regions are given in Figure 3.1.

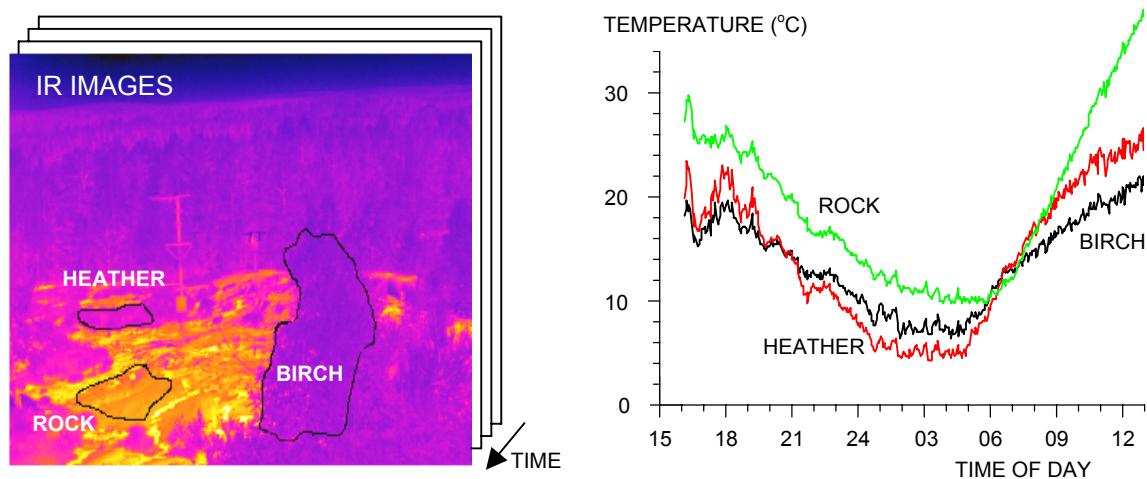


*Figure 3.1 Lined up IR images used for studying temperature variation with time. The defined areas of background elements in the image shown can be re-found in all the stacked images, and the calculated mean temperatures are presented to the right.*

## 3.2 Example calculations

### 3.2.1 General simplifications

During testing of the model, modifications were made to the general model described by the equations (2.6), to keep the calculations as simple as possible. In the following example calculations, the latent heat term was ignored as it was expected to be of little significance to the results. In order to keep the terms independent of each other the product  $\epsilon\sigma$  in the radiative term  $\epsilon\sigma T_s^4$  was replaced by  $\beta$  and treated as a separate free parameter.

To further simplify the calculations, the heat capacity  $C$  was defined to be equal to 1. This is allowed since all equations in (2.6) are linear in the model parameters. A scaling of  $C$ , therefore only implies a scaling of the other parameters.

Parameter estimation was done with time steps of both 30 second and 5 minutes. The calculations showed no significant reduction in RMS-error when 5-minute time steps were used, and consequently 5-minute time steps were chosen for the example calculations. This can be explained by the thermal inertia of the surfaces modelled. Since the temperature change of the surfaces appears to happen on a time scale of several minutes it is not unreasonable to simulate the thermal behaviour at 5-minute intervals.

### 3.2.2 Edge of forest

A very relevant background element in military context is a tree line or edge of forest. Also with respect to simulations this is a practical background element to use, because it is often difficult to select pixels representing a single tree from thermal images. Further, edge of forest can be considered to be opaque as opposed to a single tree that in this context must be considered partially transparent. The model parameters for edge of forest have been calculated on the basis of both coniferous and deciduous trees.

For the calculations for edge of forest, the conduction term has been ignored, as this term has a negligible effect on trees (except maybe tree trunks). The mathematical expression for the edge of forest calculations is given in (3.1).

$$\frac{dT_s}{dt} C = \alpha W_{\text{sun}} + \epsilon W_{\text{sky}} - \beta T_s^4 - (h_1 + h_2 v_a)(T_s - T_a) \quad (3.1)$$

Since the background element edge of forest does not have a defined orientation, the sky and sun radiation values were input to the model as the radiation sensors measured them. That is, the radiation sensors measure radiation on a horizontal surface, and no correction was done.

Examples of results for edge of forest are shown in Figure 3.2 together with actual measured temperatures. Two calculated curves are given, one with parameters optimised for the period

shown (short-term) and one with parameters optimised for data from 163 days (long-term) from spring to autumn. The short-term parameters gives good results for the period shown, but does not perform as well as the long-term parameter set for other periods.

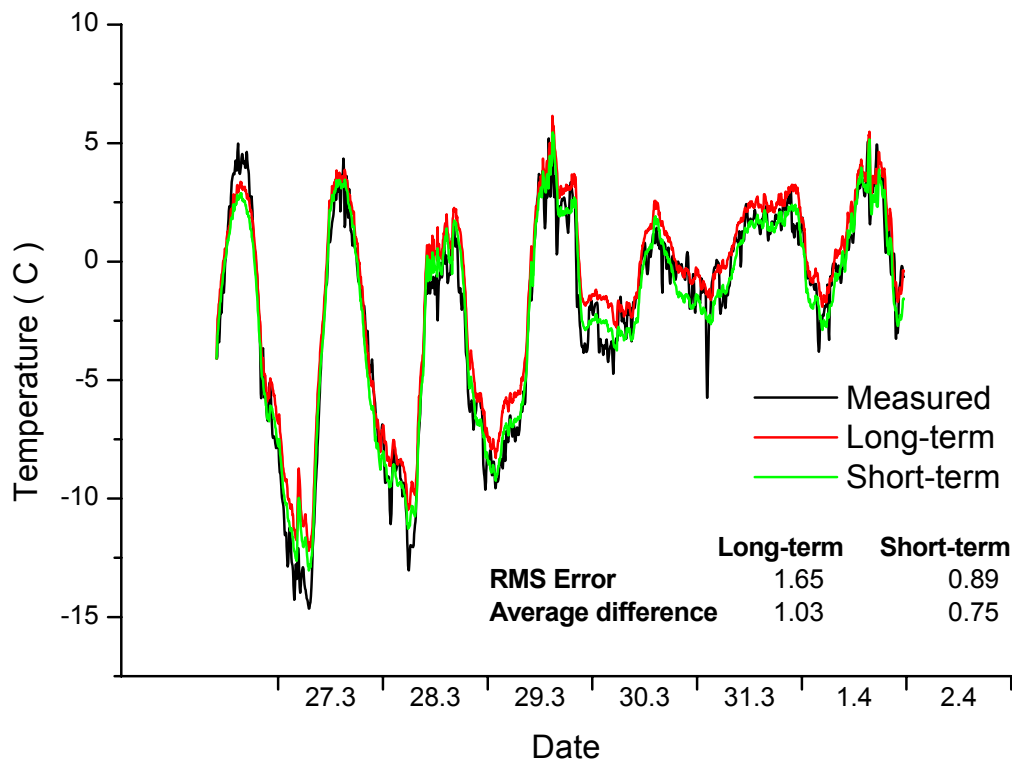


*Figure 3.2 Plot of Edge-of-forest temperatures for late March 2001, with values for average error and RMS error inserted. Two parameter sets are used: a) Long-term based on 163 days and b) Short-term based on the days shown in the figure.*

For the whole 163-day period the model gave a RMS error of 1.4K. The same model parameters have been used to predict surface temperatures for a sequence of 105 days from Bardufoss. This resulted in a RMS value of 1.9 K. However, edge of forest is probably one of the easiest background types to model, as it couples strongly to air temperature.

The average difference between the calculated and measured temperatures for the 163-day period at Rygge has been plotted in Figure 3.3. As can be seen from the plot the model accuracy degenerates rapidly for temperatures below about  $-8^{\circ}\text{C}$  (265 K). This can be explained by several factors. As the temperature drops below  $0^{\circ}\text{C}$  (approx. 273 K), icing may affect the reflective properties of the trees, and the phase changes back and forth between ice and water will absorb and liberate energy. Also, low temperatures will occur mostly during periods when there are no leaves on the deciduous trees, and a variation in leaf coverage will change the thermal properties of the background element. Finally there are fewer data containing low temperatures, meaning that the parameter estimation will weigh the lower temperatures less.

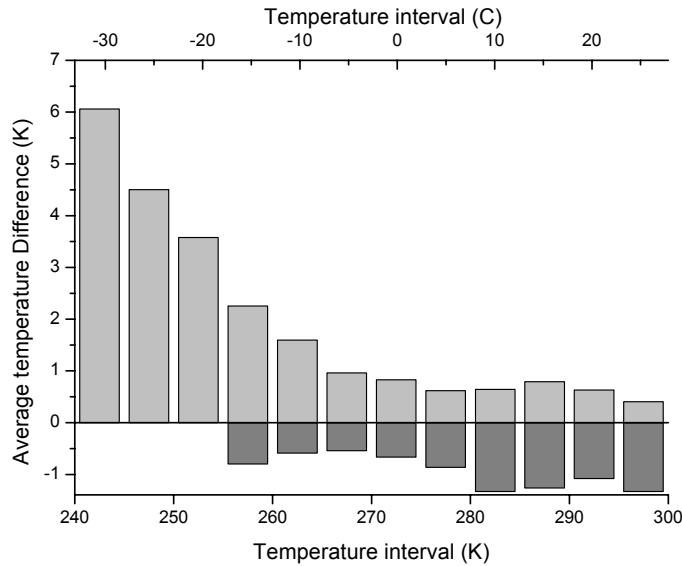


*Figure 3.3 Average difference between calculated and measured temperatures for edge of forest for a period of 163 days. Positive and negative deviations have been separated; positive values meaning calculated temperatures are too high.*

### 3.2.3 Rock

As for edge of forest (2.6) was simplified by ignoring the latent heat exchange. Modelling of the rock has been tried both with and without the conduction terms. Without the conduction terms the model performs quite well for short periods of time. However, it does not perform as well when extended beyond a few days, clearly indicating that internal conduction contributes significantly to the surface temperature.

The heat conduction is modelled by dividing the rock into 21 layers vertically. The conduction coefficient is assumed to be the same for each layer, and is assumed to be independent of the time of year, wetness etc. No assumptions are made about the thickness of the layers, other than that the lowest layer will be sufficiently deep to be at a constant temperature. This constant temperature was set to 5 °C. The initial temperature of the 21 layers is simply a linear interpolation between the initial measured surface temperature and the constant temperature of the lowest layer. This means that the model will need some time to adjust, since the initial ground profile does not contain the correct temperature history.

The results for 5 days in late March 2001 are plotted in Figure 3.4 together with measured temperatures. Two calculated curves are given, one with parameters optimised for the period shown (short-term) and one with parameters optimised for data from a period of 98 days from March to June (long-term)

As can be seen from the figure, using the long-term parameters the model has problems predicting the highest temperatures. This is probably due to the fact that these are extreme temperatures for the period upon which the model is based. The RMS error of the long-term model is 1.6 K for the entire three-month period.

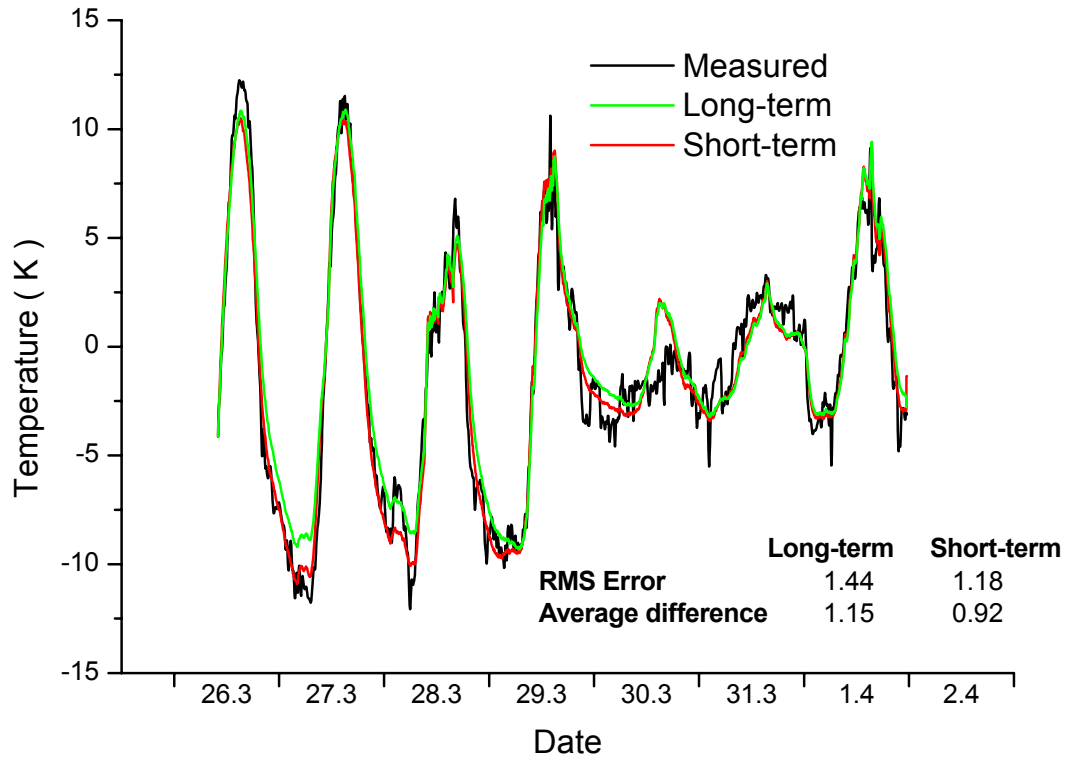


Figure 3.4 Plot of rock model for late March 2001 at Rygge with values for average difference and RMS error inserted. Two parameter sets are used: a) Long-term, based on 98 days and b) Short-term based on the days shown in the figure.

Figure 3.5 shows the average temperature difference between the calculated and measured surface temperatures for a period of approximately three months from March to June at Rygge. From the figure can be seen that the model tends to predict too high temperatures at low temperatures and too low temperatures when the surface is relatively hot. This may be

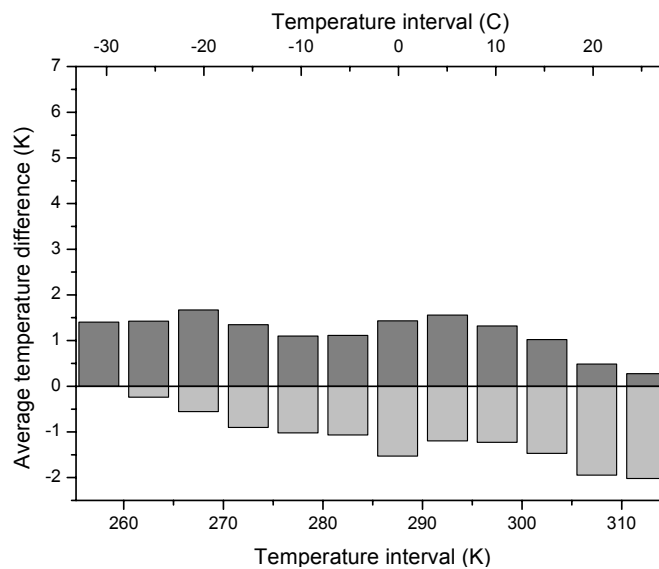


Figure 3.5 Average difference between rock model temperature and actual measurements plotted in 5-degree intervals for a period of 98 days. Positive values meaning model predicts too high temperatures.

caused by the fact that the extreme temperatures occur relatively seldom, and therefore these data points are given relatively low weight by the parameter estimation algorithm. It may also be that the model ignores heat transport processes that are significant in extreme temperature situations, and thus fails to predict the extreme situations correctly. This will be explored in the ongoing development of the model.

### 3.2.4 Model parameters

The model described by (2.6) is based on the physical processes that govern the temperatures of natural surfaces, although a number of simplifications have been made. A good indication that the simplifications are justified is when the estimated model parameter values are physically reasonable.

As discussed in paragraph 3.2.1 the heat capacity  $C$  was set equal to 1 for the example calculations and thereby scaling all parameter values correspondingly. To get an estimate of the unscaled, “true”, parameter values assumptions have to be made about one of the model parameters. The natural choice is to fix the emissivity, because this value is fairly constant for the surfaces considered, and  $\varepsilon = 0.95$  is a reasonable choice (7)(8).

As can be seen from Table 3.1 the parameters take values that seem physically reasonable. There are no negative parameters, which would imply cooling of the background element when energy is added.

Parameter	Edge-of-forest		Rock	
	Model Value	Modified value	Model Value	Modified value
$\alpha$	1.05E-05	0.48	3.43E-06	0.71
$\varepsilon$	2.07E-05	<b>0.95</b>	4.59E-06	<b>0.95</b>
$h_1$	9.80E-04	44.99	1.89E-06	0.39
$h_2$	5.32E-04	24.43	1.26E-05	2.6
$\sigma$	1.79E-12	8.65E-08	2.94E-13	6.42E-08
$\kappa$	N/A	N/A	8.81E-05	18.24

Table 3.1 Model parameter values.  $\varepsilon$  is fixed at 0.95.

The short wave absorptivity coefficient  $\alpha$  is between 0 and 1. This value represents the effective solar absorptivity and is the integrated spectral absorptivity weighted with the solar spectrum. Typical values for vegetation is 0.65 – 0.85 (Norwegian green camouflage colours), and the calculated parameter value for edge of forest is 0.48. A possible explanation for this deviation is that the values in literature refer to the properties of plane surfaces and at small angles of observation. In the case of edge of forest the surface is not plane, and the angle of incidence is not well defined because of the leaf orientation distribution. Nonetheless, the value 0.48 is considered physically reasonable. For rock the value  $\alpha = 0.71$  is within the values found in literature (Norwegian camouflage colour gray has  $\alpha = 0.75$ ).

No values for the parameters for free and forced convection have been found in literature, but it can be seen from the table that the convection parameters for edge of forest are much higher than the parameters for rock. This is reasonable since edge of forest or vegetation has a much

more structured surface than the relatively flat and smooth rock surface used in the calculated example, and therefore couple more strongly to air temperature.

Although  $\sigma$  in the model equations is a constant (Stephan-Boltzmann's constant,  $5.67\text{E-}08 \text{ Wm}^{-2}\text{K}^{-4}$ ), it has been treated as a free parameter in the example calculations. A good indication that the model is physically reasonable would then be if  $\sigma$  could be estimated with reasonable accuracy. As Table 3.1 shows, the estimated values for  $\sigma$  are too high for both models, and the discrepancies are in the order of 10-50%. Since the radiative term represents a loss term, this indicates that some other significant loss mechanisms could be ignored in the model. The most obvious candidate is the latent heat exchange, but this has not been investigated. For a period of approximately 6 months at Bardufoss this method has, however, estimated  $\sigma$  with 1% accuracy (see Table 3.3).

### 3.3 Model results

In addition to the two background elements presented above, model parameters have been calculated for heather and gravel. The model used for these elements is similar to the rock model, that is internal heat conduction is included. Also calculations for these background elements showed good agreement with measured surface temperatures.

A summary of the results for all example calculations is presented in Table 3.2.

Background element	RMS-error (K)	Mean abs( $\Delta T$ ) (K)	# days
Edge of forest	1,4	1,1	163
Heather	1,7	1,3	24
Rock	1,6	1,3	98
Gravel	1,7	1,4	12

*Table 3.2 RMS error and mean error for calculated surface temperatures for edge of forest, rock, heather and gravel.*

### 3.4 Parameter sensitivity

As discussed in paragraph 2.3, the model parameter values are estimated by minimizing  $X^2$ . The method used does not, however, supply information about the sensitivity of the model to changes in parameter values. It may also be that the estimated parameter values represent a local minimum of  $X^2$  in parameter space.

To investigate the parameter sensitivity,  $X^2$  was calculated for different parameter values around the optimized value. The calculations were performed by varying one parameter at the time and keeping the other parameters constant at the optimized values. The results for the edge of forest are shown in Figure 3.6.

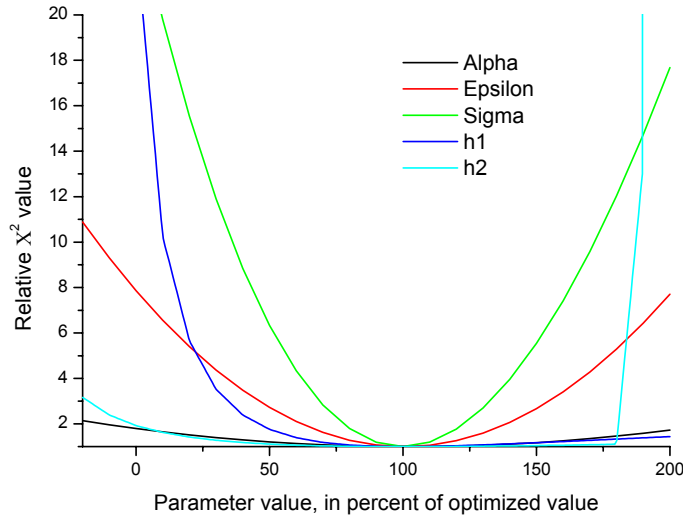


Figure 3.6 Relative  $X^2$  for the Edge-of-forest model calculated as a function of parameter value. When varying one parameter, the other parameters are kept constant at the optimised value.

The figure indicates that the absolute minimum for  $X^2$  was found. Further, it shows that the model is more sensitive to changes in some parameters than for others. It is interesting to notice that there seems to exist a critical upper value for the parameter  $h_2$  representing the forced convection.

In Figure 3.7 the relative  $X^2$  is plotted as function of the different model parameters for the rock model. Again, the figure indicates that the estimated parameters represent an absolute minimum for  $X^2$  in parameter space. It also indicates that the model is most sensitive to changes in the  $\epsilon$  and  $\sigma$  parameters.

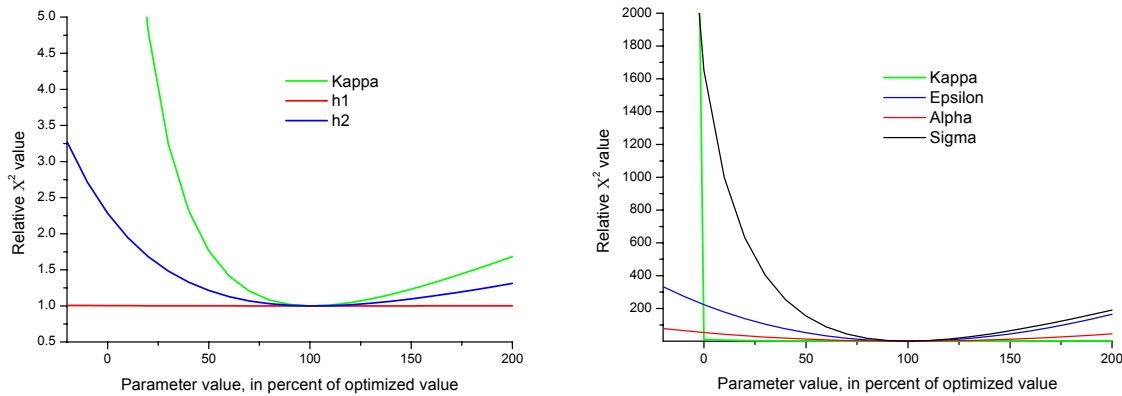


Figure 3.7  $X^2$  for the Rock calculated as a function of parameter value. When varying one parameter, the other parameters are kept constant at the optimised value.

In the examples for the rock model, a fixed core temperature at 5 °C was used, and to investigate the dependency of  $X^2$  on the core temperature  $X^2$  was calculated for different values of  $T_C$ . Figure 3.8 shows the results. A minimum for  $X^2$  appears for 5 °C, and this indicates that the other model parameters have adjusted to achieve this. This is most likely the conduction parameter  $\kappa$ , but this has to be investigated further. For a more detailed discussion, see appendix A.

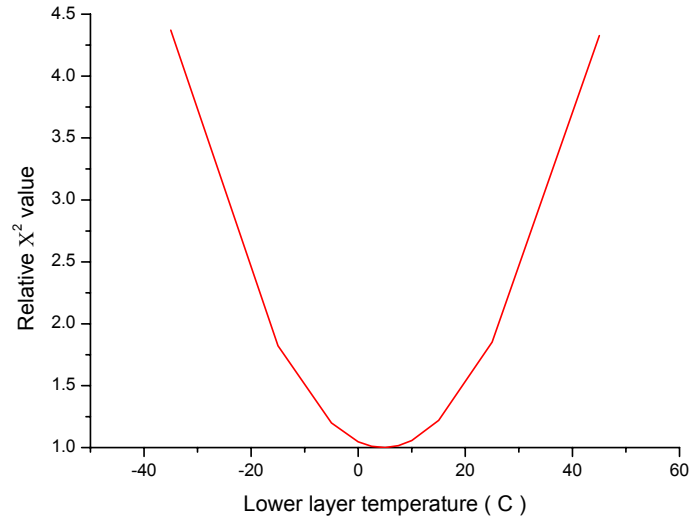


Figure 3.8  $X^2$  plotted as a function of the lower layer temperature. The other parameters are kept constant at the optimised value.

### 3.5 Model validity

Table 3.3 shows the model parameters for edge of forest calculated from both the Rygge and Bardufoss datasets.

Parameter	$\alpha$	$\varepsilon$	$\sigma$	$h_1$	$h_2$
Rygge	0.48	0.95	8.65E-08	45.0	24.4
Bardufoss	0.19	0.95	5.59E-08	13.7	4.80

Table 3.3 Edge of forest model parameter values calculated from datasets obtained at Rygge and Bardufoss. The values for  $\varepsilon$  are fixed at 0.95.

The Bardufoss parameter values differs somewhat from the Rygge parameters, e.g. the solar absorptance,  $\alpha$ , is lower at Bardufoss. The reason for this is uncertain, but may be due to the fact that the region of edge of forest in the Bardufoss imagery is sparser than at Rygge. This may also account for the differences in the other parameters. Further, the vegetation at Bardufoss is mainly deciduous, whereas at Rygge it is mainly coniferous. Therefore the trees at Bardufoss loses leaves in the autumn, and thereby the thermal properties changes.

Figure 3.9 shows the temperatures calculated for edge of forest at Bardufoss using the parameter values in Table 3.3. Calculations have been done for the period from 6 July to 16 December 2001, but only a selection of the days has been plotted in Figure 3.9.

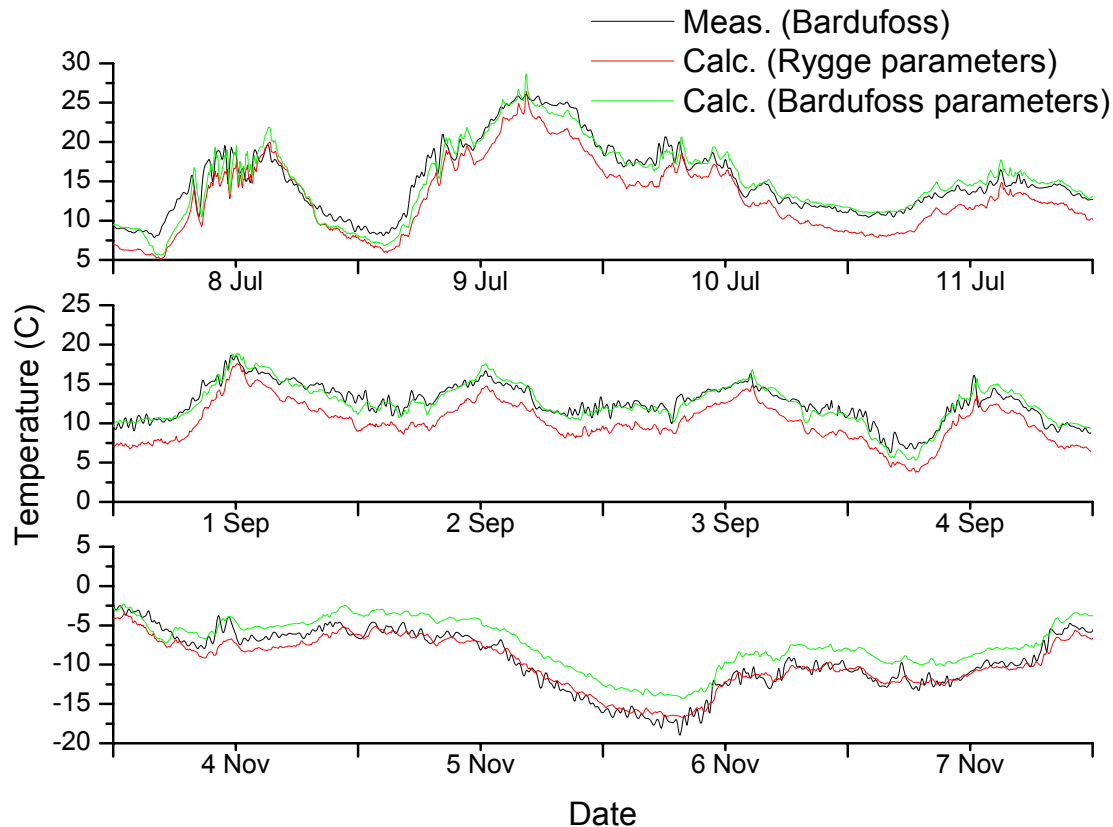


Figure 3.9 Measured temperature for three different periods at Bardufoss during year 2001 plotted together with calculated temperatures where two different sets of parameters have been used. The parameter sets have been optimised for Bardufoss and Rygge respectively. A comparison of the results using the Rygge and Bardufoss parameter values is shown in Table 3.4 below.

	RMS error	Mean abs error
Bardufoss	1,6 °C	1,3 °C
Rygge	2,2 °C	1,8 °C

Table 3.4 RMS and mean absolute error for edge of forest model with parameter values interchanged between Rygge and Bardufoss.

As shown by Figure 3.9 the Bardufoss parameters give the better results early in the period, and the Rygge parameters late in the period. This indicates that different parameter values should be used at different seasons, which is somewhat obvious since the thermal properties of the trees changes when the leaves fall.

The fact that the sets of parameters are better for different time periods indicates that the model parameters can be considered independent of geographical position, but depending on season.

### 3.6 Effect of the individual parameters

Figure 3.10 shows how the individual parameters in the model affect the surface temperatures of the background elements. The effect is plotted as the temperature change resulting from each of the parameters per model time step. The effects have been plotted for a 4-day period in

April 2001 and for a 4-day period in May 2001. The period in April is a period with cloudy weather, and the period in May is dominated by sunny weather. Measured temperature variations for edge of forest, rock and air have also been included in Figure 3.10. The modelled temperatures for rock and edge of forest are almost identical to the measured curves and are therefore not included.

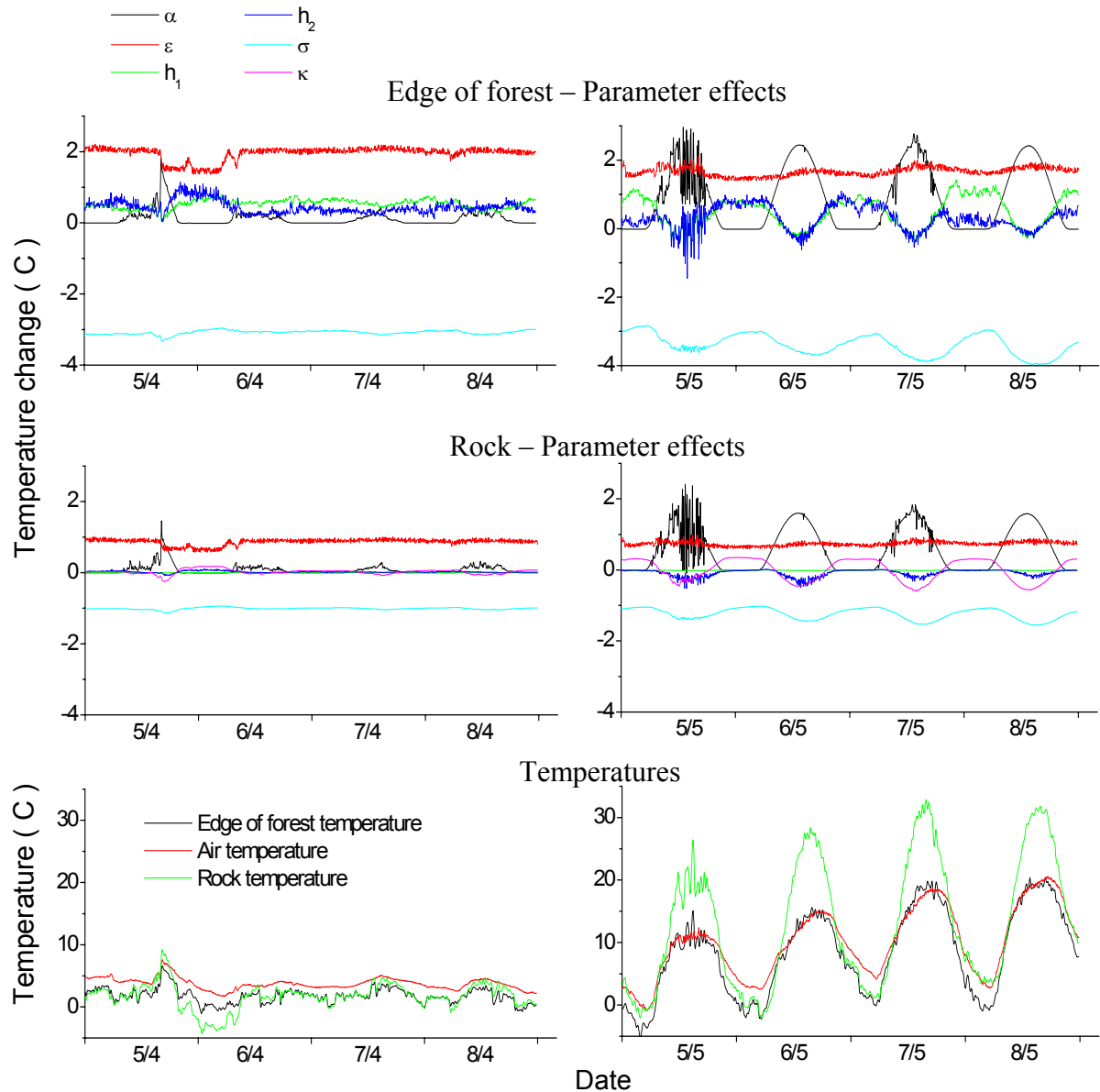


Figure 3.10 Effects of the individual parameters of the model on the surface temperature of rock and edge of forest for two 4-day periods, one with cloudy weather in April and one with sunny weather in May 2001. The effect is plotted as the temperature change in degrees Celsius per 5 minutes. In addition the measured temperature of rock, edge of forest and air are included for the same periods.

From Figure 3.10 can be seen that the edge of forest is much more affected by convection than the rock background element. This is as expected because the free and forced convection parameters are much higher for the edge of forest than for the rock model.

The temperature plots in Figure 3.10 shows that both rock and edge of forest has quite similar temperature variations for the cloudy April period. Both have roughly the same temperature variations as the air, but with a temperature of 1 to 2 degrees below that of the air. It may seem more reasonable for the background temperatures to be about the same as for the air for periods of little solar loading. However since the cloud cover usually appears “cold” the effect of the long wave irradiation will normally be smaller than the effect of the radiation emitted from a background element at air temperature. Therefore the background element will take a temperature at which the convection and radiation effects cancel each other. This suggests that for periods that are not sunny using air temperature minus one to two degrees may be a good model for both rock and edge of forest. The exact temperature difference will depend on how “cold” the sky looks and therefore on the height and type of cloud cover. It also suggests that the temperature contrast in the background will be very small for such periods.

For the sunny May-period the rock has a much higher temperature during the day than the edge of forest. This is because the rock has a higher solar absorptivity and lower convection parameters than the edge of forest as shown in Table 3.1. Also, it takes a while longer for the rock than for the edge of forest to cool down to below air temperature when the sun sets. This is due to the thermal inertia provided by the heat capacity and the heat conduction and the fact that the rock attains a higher temperature during the day than the edge of forest.

Parameter	Edge of Forest		Rock	
	May	November	May	November
$\alpha$	0.76	0.10	0.50	0.06
$\varepsilon$	1.85	1.63	0.82	0.72
h1	0.59	0.73	0.01	0.01
h2	0.35	0.59	0.07	0.07
$\sigma$	3.45	3.05	1.26	0.96
$\kappa$	N/A	N/A	0.25	0.11

*Table 3.5 Absolute average temperature change caused by the individual parameters of the model on the surface temperature of rock and edge of forest. The calculated values are based on a sunny 10-day period in May 2001 and a cloudy 6-day period in April 2001.*

The absolute average values of the effects of each parameter are presented in Table 3.5. The only parameter that seems to have a nearly negligible effect is the free convection in the rock model. All other parameters have a significant effect on the surface temperatures of the background elements. Forced convection has a very low average effect on the surface temperature for the rock model. However it has a cooling effect during periods of high solar loading. This probably prevents the model temperature from overshooting the measured temperatures during such periods.

Table 3.5 identifies the radiation parameter  $\sigma$  as the parameter having the highest impact on the surface temperatures. As can be seen from Figure 3.10 this is the only major heat loss mechanism in both models.

#### **4 SUMMARY**

A model for calculation of surface temperatures of different background elements like edge of forest, heather, rock and gravel has been developed. The model is based on a simple mathematical description of the physical processes involved in heat transfer to and from an outdoors natural surface. The same model is used for all background elements, but with different sets of model parameters.

Example calculations for edge of forest and rock have been given, showing very good agreement with measured surface temperatures. The model parameters were estimated by fitting the model to measured surface temperatures. It has been shown that all the parameters used in the model are necessary for the model to make accurate predictions for long periods of time. Finally, the model sensitivity to changes in model parameters have been discussed and it has been demonstrated that the model performs well even with model parameters estimated from data obtained from different geographical locations.

## APPENDIX

### A HEAT CONDUCTION

The model calculates heat conduction by dividing the background elements into 21 layers of undefined thickness. The undefined layer thickness is a consequence of the mathematical formulation of the problem, and it complicates the comparison of calculated and measured temperature profiles. This section describes how the model handles heat conduction and gives a method for comparison of calculated and measured temperature profiles.

At the measuring sites there were recorded measurements of the temperature in the ground at 2, 10, 20 and 30 cm depth. A rock temperature sensor designed specifically for this purpose performed these measurements. The rock background element was modeled on a patch of bare rock where such a sensor was placed. It is therefore interesting to compare the heat conduction in the model, e.g. the temperatures of all the layers, with measurements from the rock temperature sensor. An example of temperatures measured at different depth in rock is shown in Figure A.1.

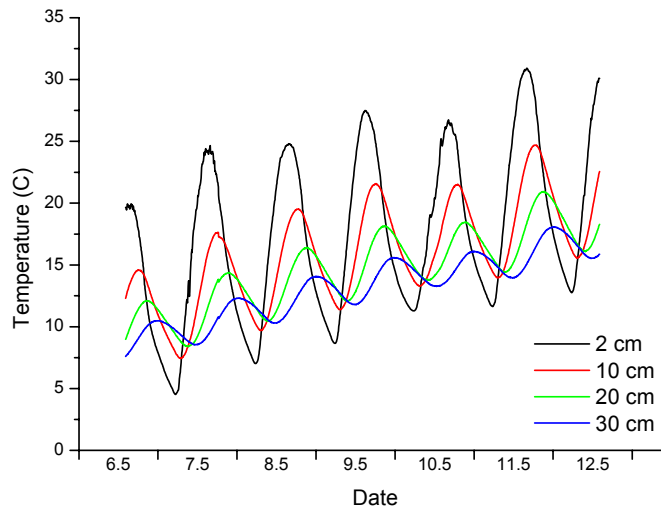


*Figure A 1* Temperatures measured in rock for four different depths, in May 2001. This dataset is the basis for the calculations performed in section A.4.

Because the thickness of the model layers is undefined, temperatures cannot be compared directly, but thermal diffusivity and the damping depths must be compared. The calculations of these parameters are best done for a period for which the surface temperatures vary as close to sinusoidal as possible, because this allows the use of very simple formulas for damping depth and thermal diffusivity. On a daily basis the temperature will be close to sinusoidal for periods of relatively constant weather close to the solar equinoxes.

#### A.1 Difference formulae for heat conduction

The calculation of heat conduction in the model is based on Fourier's heat conduction equation, which is presented in (A.1) below.

$$\frac{dT}{dt} = \frac{1}{\rho \cdot c} \nabla(\lambda \cdot \nabla T) \approx \alpha_h \cdot \frac{\partial^2 T}{\partial z^2} \quad (\text{A.1})$$

$$\alpha_h = \frac{\lambda}{\rho \cdot c}$$

In (A.1)  $\rho$  is the density,  $\lambda$  is the conductivity,  $c$  is the specific heat capacity,  $\alpha_h$  is the thermal diffusivity,  $T$  is the temperature and  $t$  is the time.

Heat conduction in the ground can usually be assumed to be one-dimensional. In some cases a thermal diffusivity that is constant with depth and time can also be assumed. These two conditions give the approximation in equation (A.1). The latter assumption may not always be correct, especially for soil in which the thermal diffusivity will depend on the fractions of soil constituents and water content. For solid rock, however, it should be a good approximation.

The model is divided into 21 layers of equal unspecified thickness  $\Delta z$ , and a temperature is calculated for each layer for discrete time intervals  $\Delta t$ . The lowest layer is set to a constant temperature of 5 °C. Fourier's heat conduction equation is converted from a differential equation to a difference equation by using a first order approximation. This is shown in (A.2).

$$\begin{aligned} T_i(t + \Delta t) &= \left( e^{\frac{\Delta t}{\alpha_h}} \right) T_i \approx \left( 1 + \Delta t \frac{d}{dt} \right) T_i = \left( 1 + \alpha_h \cdot \Delta t \frac{\partial^2}{\partial z^2} \right) T_i \approx \left( 1 + \alpha_h \cdot \frac{\Delta t}{\Delta z^2} \delta_0^2 \right) \cdot T_i \\ &= T_i + \frac{\alpha_h}{\Delta z^2} \cdot (T_{i+1} - 2T_i + T_{i-1}) \cdot \Delta t \\ &= T_i + \frac{1}{2} \kappa \cdot (T_{i+1} - 2T_i + T_{i-1}) \cdot \Delta t \end{aligned} \quad (\text{A.2})$$

In (A.2)  $\delta_0$  is the central difference operator and  $T_i(t)$  denotes the temperature of layer number  $i$  at time  $t$ . The model performs the calculation as shown in the final line of (A.2) estimating the parameter  $\kappa$ . Equation (A.2) gives a formula for calculating all the layer temperatures except for the upper layer. The upper layer is exposed to the surroundings, exchanging energy through different processes including conduction from the layer below. According to Rønning (9) a first order approximation to the heat equation for this layer is not sufficiently accurate. He suggests calculating the surface temperature by considering the heating of a layer of thickness  $\frac{1}{2}\Delta z$ , just below the surface.

If  $G_0$  is the power flux per square meter at the surface, caused by other sources than heat conduction and  $T_s$  is the surface layer temperature this gives equation (A.3).

$$\frac{1}{2} \Delta z \cdot \rho \cdot c \cdot \frac{T_s(t + \Delta t) - T_s}{\Delta t} = G_0 + \frac{\lambda \cdot (T_1 - T_s)}{\Delta z} \quad (\text{A.3})$$

Solving (A.3) for the surface temperature at time  $t + \Delta t$  gives (A.4).

$$\begin{aligned}
T_s(t + \Delta t) &= T_s + \left( \frac{G_0}{\frac{1}{2} \Delta z \cdot \rho \cdot c} + \frac{2\alpha_h}{(\Delta z)^2} \cdot (T_1 - T_s) \right) \cdot \Delta t \\
&= T_s + [g_0 + \kappa \cdot (T_1 - T_s)] \cdot \Delta t
\end{aligned} \tag{A.4}$$

The last line in (A.4) shows how the calculations are implemented in the model. The parameter  $\kappa$  is the same parameter as in (A.2), while  $g_0$  includes parameters for all other influences on the surface layer temperature.

## A.2 Heat conduction with sinusoidal temperature variations

Assuming that the temperature  $T_s$  on the rock surface has a sinusoidal variation about a mean temperature  $T_m$  with an angular frequency  $\omega$  and with a thermal diffusivity independent of depth, gives (A.5).

$$\begin{aligned}
T_s &= T_m + A_s \cdot \sin[\omega \cdot (t - t_m)] \\
T(z = 0) &= T_s \\
T(z) &\xrightarrow{z \rightarrow \infty} T_m
\end{aligned} \tag{A.5}$$

In (A.5)  $t_m$  is the time at which  $T_s = T_m$ . The second and third lines in (A.5) represent the boundary conditions. Solving Fourier's heat conduction equation for  $T(z)$  with the conditions in (A.5) results in (A.6).

$$\begin{aligned}
T(z) &= T_m + A(z) \cdot \sin\left(\omega \cdot (t - t_m) - \frac{z}{z_d}\right) \\
A(z) &= A_s \cdot e^{-\frac{z}{z_d}}
\end{aligned} \tag{A.6}$$

$$z_d = \sqrt{\frac{2\alpha_h}{\omega}}$$

Using this equation it is possible to calculate the damping depth  $z_d$  given the amplitude at two depths  $z_1$  and  $z_2$ , as shown in (A.7).

$$z_d = -\frac{\Delta z}{\ln[A(z_2)/A(z_1)]} \tag{A.7}$$

$$\Delta z = z_2 - z_1$$

This result is only valid for a material with a constant thermal diffusivity and with a perfectly sinusoidal variation of the surface temperature. The latter condition will normally not be fulfilled, but for periods when the day length is close to 12 hours it will be a good approximation for the daily temperature variations. This also requires fairly constant weather

conditions, at least for a few days. In this case  $\omega$  takes the value  $\omega_{\text{daily}} = 2\pi/86400$  with the time  $t$  in seconds.

Equations (A.6) and (A.7) can also be applied to the annual temperature variations, but with a different value for the angular frequency. Using weekly average temperatures and an angular frequency  $\omega_{\text{annual}} = \omega_{\text{daily}}/365$  gives the damping depth for the annual temperature variations,  $z_d^{\text{annual}}$ . This is shown in (A.8).

$$z_d^{\text{annual}} = \sqrt{365} \cdot z_d \quad (\text{A.8})$$

### A.3 Calculation of damping depth based on measurements by the rock temperature sensor

To calculate the damping depth it is necessary to estimate the amplitude of the daily temperature variations at several depths in the rock. Calculating the amplitude ratio between two different depths then gives the damping depth, as shown in (A.7). However, it is not straightforward to measure the temperature amplitude because the temperature variations are not sinusoidal, as can be seen from figure A.1.

A period of 6 days, starting at 14:10 May 6 2001 were chosen as the data basis for performing these calculations. These days were dominated by clear weather that remained fairly constant throughout the entire period, thereby resulting in nearly sinusoidal temperature curves, even though the day length of the period was close to 17 hours.

Subtracting a daily moving average from the plot shown in Figure A.1 results in curves that are much closer to sinusoidal. The moving average is an average of the 12 hours before and the 12 hours after the measurement. I.e. from each measurement is subtracted the daily temperature average. The result of this operation is shown in Figure A.2.

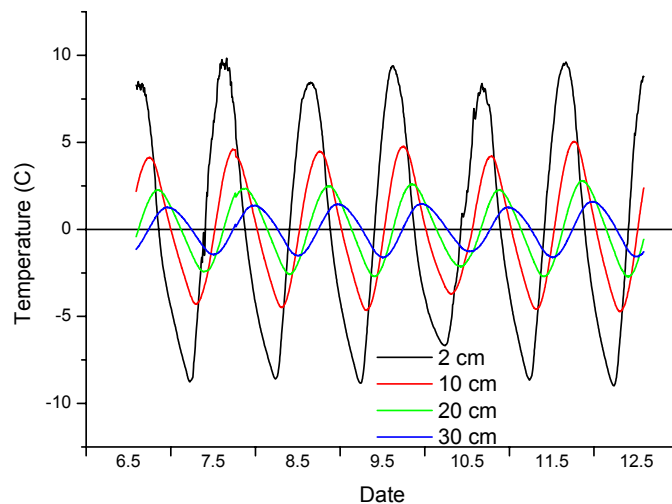


Figure A.2 Temperatures measured in rock for four different depths, in early May 2001. A daily average temperature for each of the depths has been subtracted.

The plots in Figure A.2 are still not entirely sinusoidal, but are a close approximation. Fitting a sine curve to the temperature curve at 30 cm depth gave an RMS error of only 13% of the amplitude.

Taking the absolute values of the curves in figure A.2 and averaging over the entire 6 day period gives an estimation of the ratios of average amplitudes. This operation is shown in (A.9).

$$\frac{A(z_2)}{A(z_1)} \approx \frac{\langle |T(z_2) - T_{Avg}(z_2)| \rangle}{\langle |T(z_1) - T_{Avg}(z_1)| \rangle} \quad (\text{A.9})$$

In (A.9)  $\langle Y \rangle$  denotes averaging  $Y$  over the entire 6 day period,  $|Y|$  the absolute value of  $Y$ ,  $T(z)$  is the temperature at depth  $z$  and  $T_{Avg}(z)$  is the daily moving-average temperature at depth  $z$ . Inserting this value into equation A.3 gives an estimate of the daily damping depth and thermal diffusivity of the rock,  $z_d \approx 18$  cm,  $\alpha_h \approx 1.2 \cdot 10^{-6}$  and  $z_d^{\text{annual}} \approx 3.5$  m

#### A.4 Calculation of damping per layer

The damping factor can also be calculated for the rock model. However, for the model the thickness per layer is not specified, and it is therefore not possible to calculate the thermal diffusivity or conductivity. The only calculation that can be made is the damping per layer, but if this is compared to the damping depth derived from the temperature measurements, it is possible to give an indication of the layer thickness, even though the layer thickness is of no consequence to the model.

The data used for calculating the damping is the temperature curve for each layer in the model, for a six-day period in May 2001. The temperature curves were modified by moving averages, in the same way as described in section A.3. The amplitude ratios  $A_i/A_{i-1}$ , where  $i$  is the “layer number” with the surface as 0 and the lowest layer as 20, have been calculated. The result has been plotted in figure A.3.

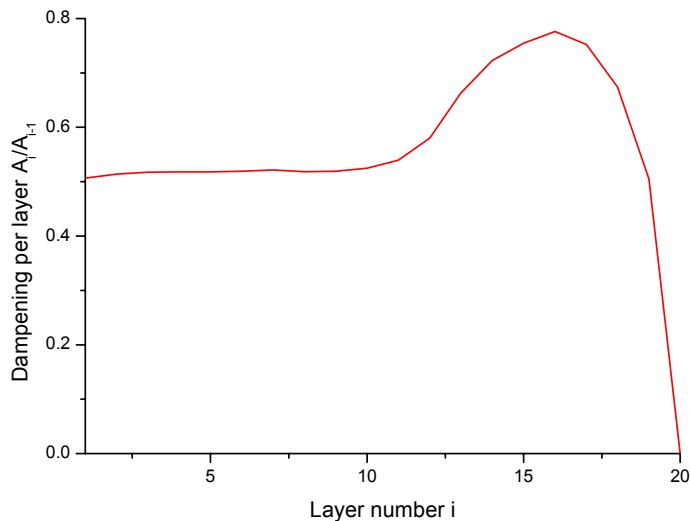


Figure A.3 Dampening per layer in rock model, as a function of layer number  $x$ , where the damping is calculated as the amplitude ratio between layers no.  $i$  and  $i-1$ .

For the first 10 layers the damping is approximately 50 % per layer, but below the 10<sup>th</sup> layer the calculated damping changes. The reason for this is that the moving average subtraction does not result in sinusoidal curves for layers deeper than about the 10<sup>th</sup> layer. Therefore this method cannot be used to calculate amplitude ratios for layers 11 to 20.

Damping of the annual thermal wave can then be calculated as shown in (A.8). This gives a damping of about 50 % for 19 layers, which means that the 20 layers used in the model is not enough to properly simulate the annual thermal wave. However this is probably not very important for the model, as the most important effect of introducing heat conduction is to enforce a thermal inertia on the background element.

Finally, comparing the damping per layer in the model to the damping depth calculated for the rock temperature sensor can give an indication of the thickness per layer. This is calculated by (A.7), and results in a layer thickness of 12 cm, the lowest layer then being at 2.4 m depth.  $z_d^{\text{annual}}$  was calculated to 3.5 meters in section A.3. The amplitude will be reduced to about 5 % of the surface value at a depth equal to three damping depths. Therefore the annual thermal wave needs roughly 10 meters of depth to be reduced to 5% of the annual surface fluctuations.

To improve the accuracy of the heat conduction modeling it may be necessary to use as much as 100 layers. Some improvement may also be achieved by using data from the rock temperature sensors to construct a proper starting profile for the temperatures in all the layers. Since the daily temperature variations is completely dampened out in about 10 layers it may be possible to use only 20 to 30 layers, but with the lowest layer having a sinusoidal temperature variation with a period of one year. In that case, the characteristics of this function may be deduced from the rock temperature sensor measurements.

## References

- (1) Olsen F B, Gamborg M, Høimyr M, Strømman E, Søderblom M(2001): Thermal signatures from objects and backgrounds – Final report project 775 (in Norwegian), FFI/RAPPORT-2001/05210
- (2) Leidner L, Clement D, Jessen W (1992): A new thermal background model and its application to BEST TWO data analysis, FGAN-FfO 92/24, FGAN-FfO.
- (3) Strømman E, Høimyr T, Gamborg M, Olsen, F B (2001): An automatic station for measurement of meteorological parameters and thermal signatures, FFI/RAPPORT-2001/05402
- (4) J.L. Monteith, M.H. Unsworth (1990): Principles of Environmental Physics, Edward Arnold1, London, 223-230.
- (5) Marco S. Cacceci, William P. Cacheris (1984): Fitting Curves to Data. The Simplex algorithm is the answer, BYTE, May 1984, 340-362.
- (6) William H. Press et al (1992): Numerical recipes in C: the art of scientific computing, Cambridge University Press, Cambridge, 408-412.
- (7) David M. Gates (1980): Biophysical Ecology In: *Springer advanced texts in life sciences* (Ed David E. Reichle), Springer-Verlag, New York, 164.
- (8) William L. Wolfe, George J. Zissis (1978): The Infrared Handbook, Office of Naval research, Department of the Navy, Washington DC, 3-90 - 3-96.
- (9) Rønning, Arne Th (1977): A one-dimensional model for calculation of soil temperatures, F-320, FFI

## DISTRIBUTION LIST

**FFIE**                      **Dato:** 10. desember 2002

RAPPORTTYPE (KRYSS AV)		RAPPORT NR.	REFERANSE	RAPPORTENS DATO	
<input checked="" type="checkbox"/> RAPP	<input type="checkbox"/> NOTAT	<input type="checkbox"/> RR	2001/05324	FFIE/775/119.2	10. desember 2002
RAPPORTENS BESKYTTELSESGRAD			ANTALL EKS UTSTEDT	ANTALL SIDER	
Unclassified			35	31	
RAPPORTENS TITTEL			FORFATTER(E)		
MODELLING THE THERMAL SIGNATURE OF NATURAL BACKGROUNDS			OLSEN Frode Berg, GAMBORG Marius		
FORDELING GODKJENT AV FORSKNINGSSJEF			FORDELING GODKJENT AV AVDELINGSSJEF:		
Stian Løvold			Johnny Bardal		

### EKSTERN FORDELING

### INTERN FORDELING

ANTALL	EKS NR	TIL	ANTALL	EKS NR	TIL
1		NOBLE	9		FFI-Bibl
1		Maj S Johansen, FO/HST	1		FFI-ledelse
1		OK B Isfeldt, FLO/SJØ-T-KSA	1		FFIE
1		Kapt T E Nicolaysen, LUKS/LKKI/LSR/BFTS	1		FFISYS
1		Kapt L V Strædet, LUKS/BBSI	1		FFIBM
1		Kapt J I Jakobsen, FLO/LAND/V.1	1		FFIN
1		Lt N Toverud, FLO/LAND/V.1	1		T Høimyr, E
1		Lt O Skaaden, VSIV/INGR	1		E Strømman, E
1		Dosent A A Grimnes, NLH PB 5065, 1432 ÅS	1		M Søderblom, E
2		ITAS, Saghellinga A, 1432 Ås	2		Forfattereksemplar(er)
2		Dr D Clement, FGAN-FOM Gutleuthausstr 1, D-76725 Ettlingen	3		Restopplag til Biblioteket
1		Dr P Jacobs, TNO-FEL PB 96864, 2509 JG den Haag The Netherlands			<b>Elektronisk fordeling:</b>
1		Mr R Balma, National Defence Headquarters, DSSPM-CCD 3-7, MGen George Parkers Building, Ottawa, Ontario K1A 0K2, Canada			FFI-veven
					Stian Løvold (StL)
					Nils A Sæthermoen (NAS)
					Egil Bingen (EgB)
					Torbjørn Skauli (TSk)
					Bjarne Haugstad (BjH)
					Stein Grinaker (SGr)
					Einar Østevold (EiO)